CHAPTER IV
RESULTS AND DISCUSSION

4.1 Formation of Porous Structure

The formation of porous structure in LDPE/starch films essentially depends on the amount of starch removed from the film matrix. Three methods have been reported to determine the level of starch remaining in/removing from the LDPE/starch film, i.e. chemical analysis, thermogravimetric analysis (TGA), and fourier transform infrared spectroscopy (Nakatsuka and Andrady, 1992). For a simple, rapid determination of weight loss, a five decimal place digital balance (Sartorious) was used for this study.

4.1.1 Acidic Hydrolysis

4.1.1.1 Effect of Acid Type

Figure 4.1 shows percentages of starch hydrolyzed from 50 μm thick films containing 12 wt% starch using 5 N HCl, 5 N H_2SO_4, 5 N HNO_3, and distilled water at 65°C as a function of time. The film immersed in water at 65°C as a control sample showed no weight loss during the test. This implies that water took no part in starch removal by aqueous acid solutions. Therefore, percentage starch hydrolysis was determined from Equation 4.1:

$$\%\ \text{starch removal} = \frac{\%\ wt\ loss}{initial\ \%\ starch} \times 100 \qquad (4.1)$$

where % starch removal is the percentage of starch hydrolysis or starch removal by acid solution, % wt loss is the percentage of weight after hydrolysis, and initial % starch is the initial percentage of starch present in the film samples.

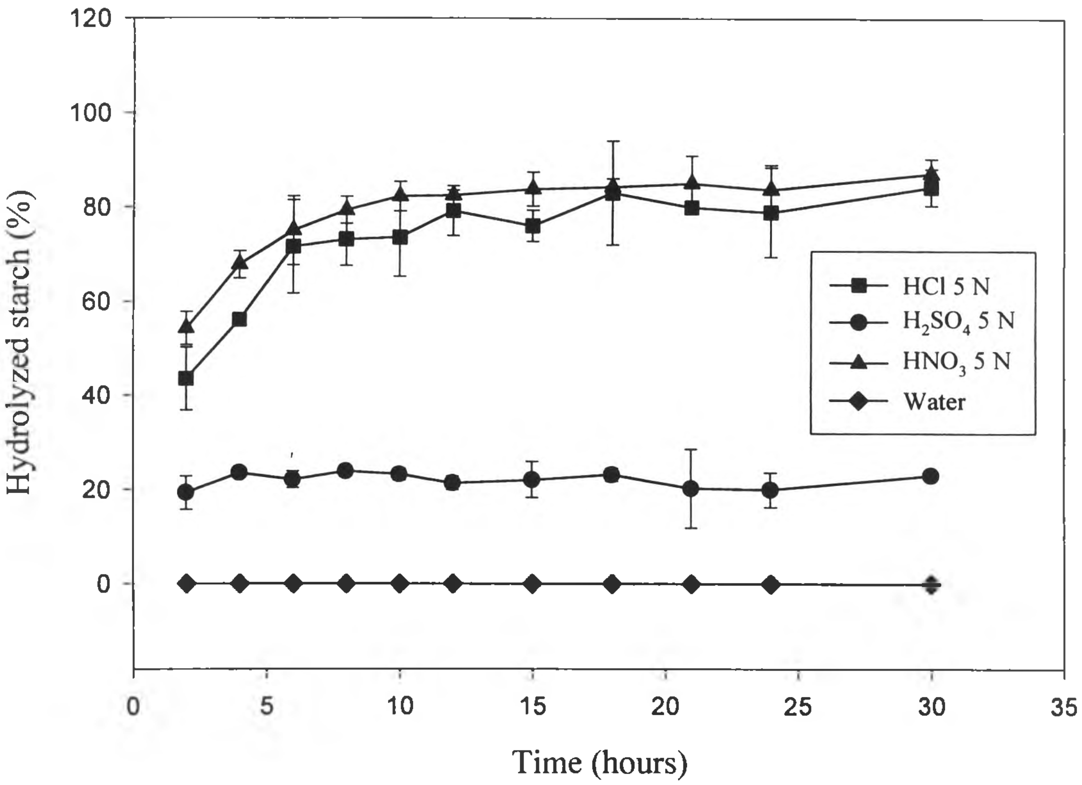

Figure 4.1 Percentages of starch hydrolysis of 50 μm thick films containing 12 wt% starch hydrolyzed in 5 N HCl, 5 N H_2SO_4, 5 N HNO_3, and distilled water at 65°C as a function of time.

Comparison of starch reductions by three types of acid solutions indicates that starch was best removed by HNO_3 solution owing to its properties as a very strong acid and a powerful oxidizer (Clarke and Mazzafro, 1993). It was observed that the percentages of starch hydrolyzed when using both HCl, and HNO_3 increased rapidly during the first 6 hours then remained constant after 8-10 hours. The reductions in starch content by HCl and HNO_3 solutions were approximately 75% and 85% respectively. On the other hand, no rapid increase in weight loss was observed for the H_2SO_4 hydrolyzed film. The film showed a reduction in starch level of only about 20%. The measurement of weight loss correlated well with the SEM micrographs shown in Figure 4.2.

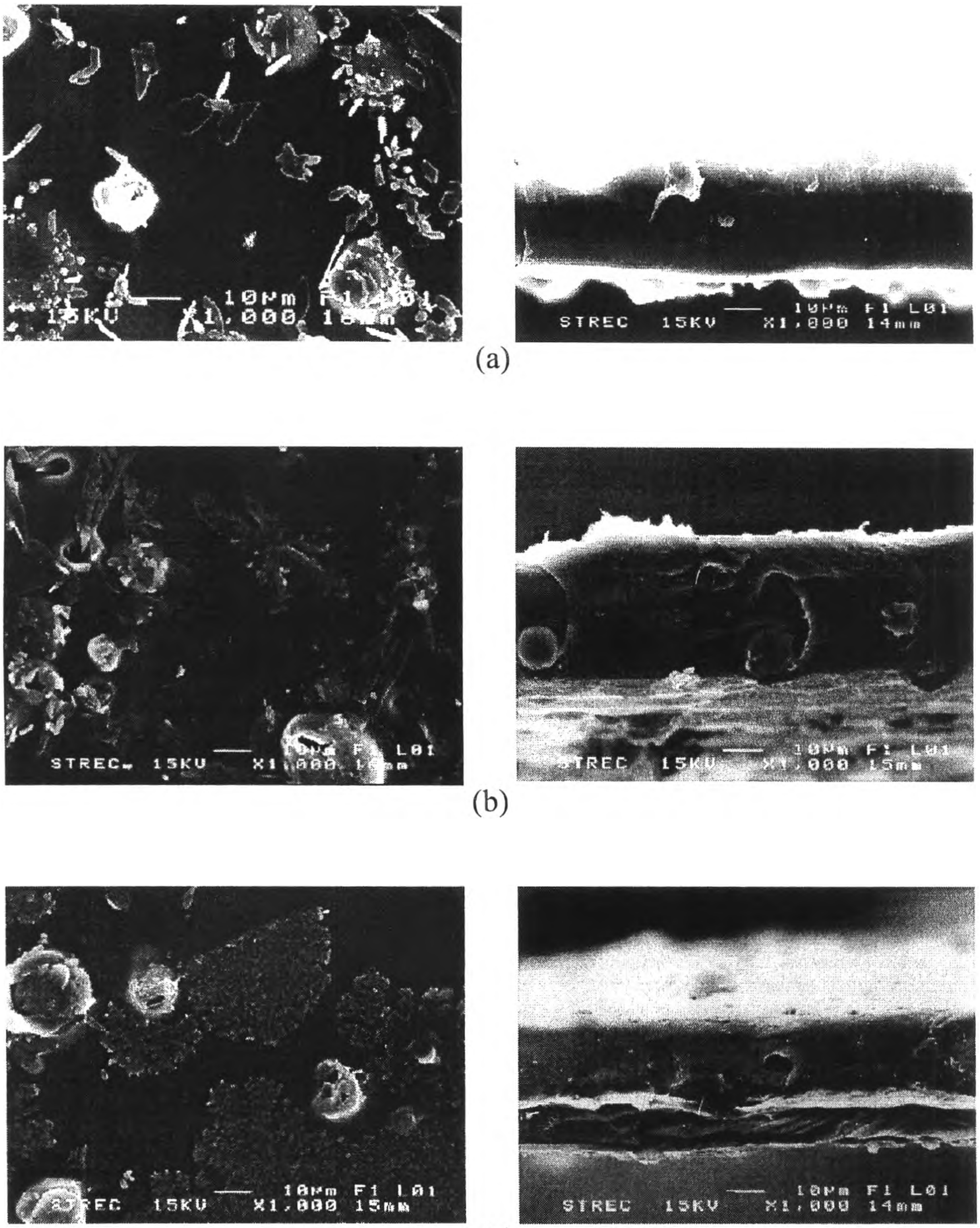

(a)

(b)

(c)

(cont.)

Figure 4.2 SEM micrographs of 50 μm thick films containing 12 wt% starch hydrolyzed in (a) distilled water, (b) 5 N HCl, (c) 5 N H_2SO_4, and (d) 5 N HNO_3 at 65°C.

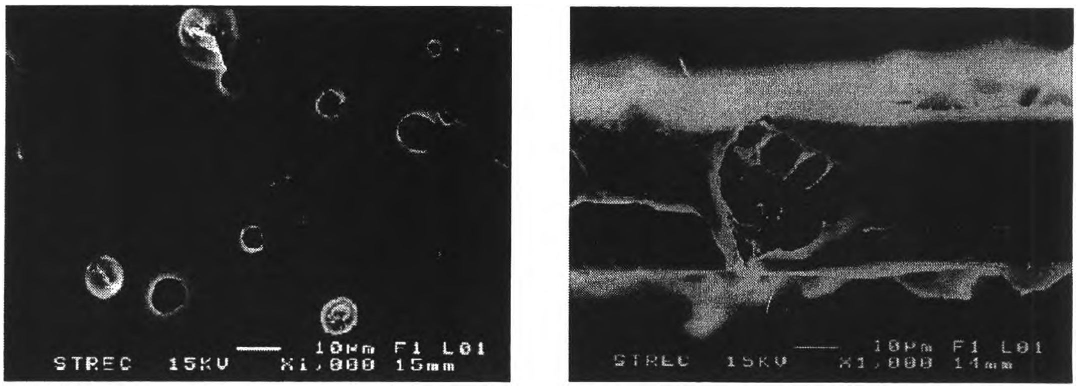
STREC 15KV 10µm F1 L01 X1,000 15mm
STREC 15KV 10µm F1 L01 X1,000 14mm

(d)

Figure 4.2 (continued)

The five SEM micrographs on the left were taken at the surfaces of the films while those on the right are the cross-sectional images. Both the surface and the cross-section of the film after immersion in water at 65°C exhibited nonporous structure (Figure 4.2a). The films hydrolyzed in HCl and H_2SO_4 solutions showed less pores on the surfaces and cross-sections (Figure 4.2b and Figure 4.2c) compared with the film immersed in HNO_3 solution (Figure 4.2d). More starch residues were also found in both HCl and H_2SO_4 hydrolyzed films than that found in HNO_3 hydrolyzed film.

4.1.1.2 Effect of Concentration

Reductions in starch contents of 50 µm thick films containing 12 wt% starch immersed in 1 N, 3 N, and 5 N HNO_3 at 65°C are given in Figure 4.3. The films hydrolyzed in 1 N, 3 N, and 5 N HNO_3 showed starch removal of about 30%, 60-75%, and 85%, respectively. This indicates that starch reduction increases with increasing concentration of HNO_3.

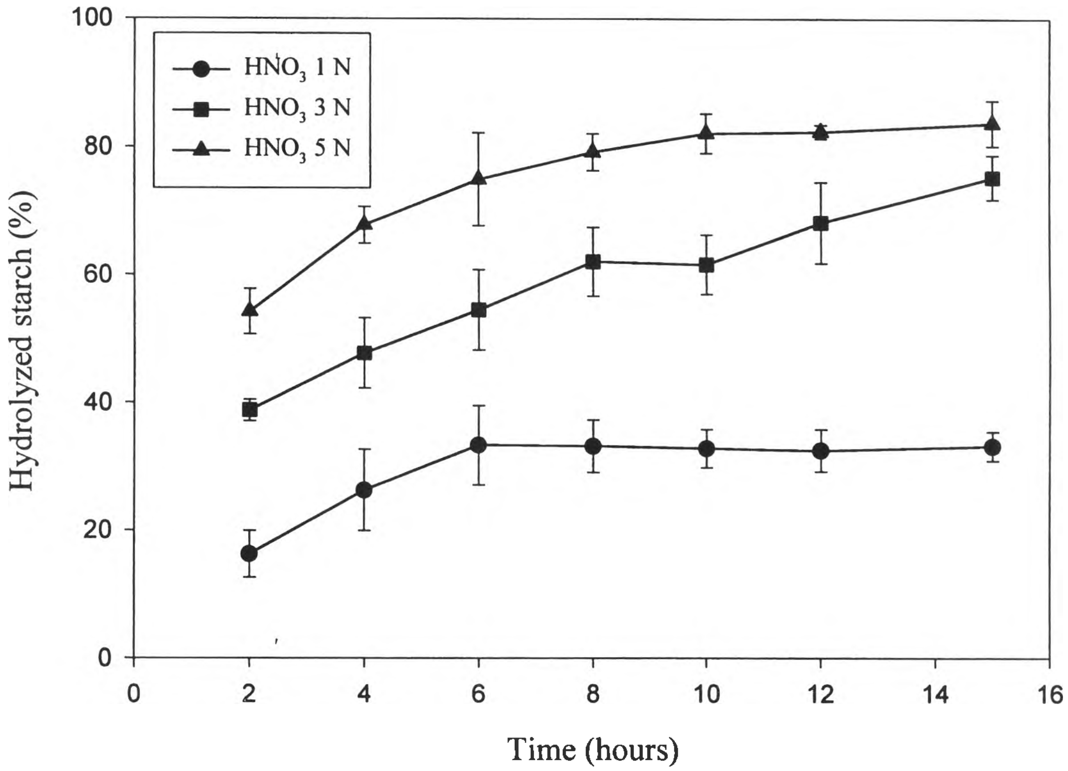

Figure 4.3 Percentages of starch hydrolysis of 50 μm thick films containing 12 wt% starch f hydrolyzed in 1N, 3 N, and 5 N HNO_3 at 65°C as a function of time.

4.1.1.3 *Effect of Temperature*

Temperature also played a vital role in acidic hydrolysis as shown in Figure 4.4. The irreversible swelling temperature range or gelatinization temperature of tapioca starch is 58.5°C-70°C (Kirk-Othmer, 1997). The action of aqueous acid solution at temperatures below the gelatinization point causes the starch particles to degrade but with little change in the external form of the particles (Whistler *et al.,* 1984). During gelatinization, starch crystallites melt and some linear amylose molecules are leached out of the starch particles into the surrounding solution. From Figure 4.4, starch reduction at 25°C and 45°C were only about 28% and 50%, respectively, whereas starch removal at 65°C gave higher values up to 85%. Therefore, starch particles were most effectively hydrolyzed at temperatures within the gelatinization temperature range of tapioca starch.

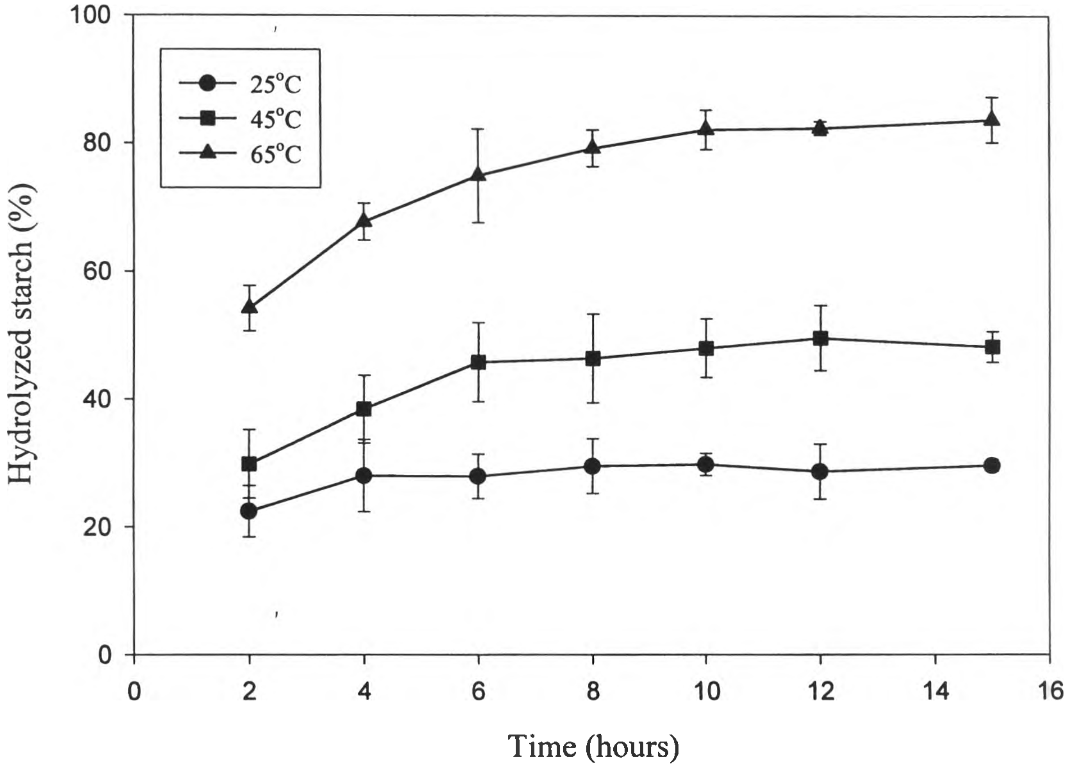

Figure 4.4 Percentages of starch hydrolysis of 50 μm thick films containing 12 wt% starch hydrolyzed in 5 N HNO_3 at 25°C, 45°C, and 65°C as a function of time.

4.1.1.4 Effect of Starch Content

Figure 4.5 shows reductions in starch content of 50 μm thick films containing 0-12 wt% starch hydrolyzed in 5 N HNO_3. All film samples were hydrolyzed in the solution for 15 hours at 65°C before weight checking. It was observed that the film containing 0 wt% starch, or pure LDPE film, exhibited no weight loss after hydrolysis. This was due mainly to the chemical resistant property of LDPE. Thus, the weight loss in LDPE/starch film was contributed by starch reduction only. When starch levels increased from 0 wt% to 12 wt%, the percentages of hydrolyzed starch was seen to increase significantly. This was thought to be because when films contain higher starch contents, the starch particles are closer together or even interconnected, thus providing more sites for hydrolysis and making solution penetration easier.

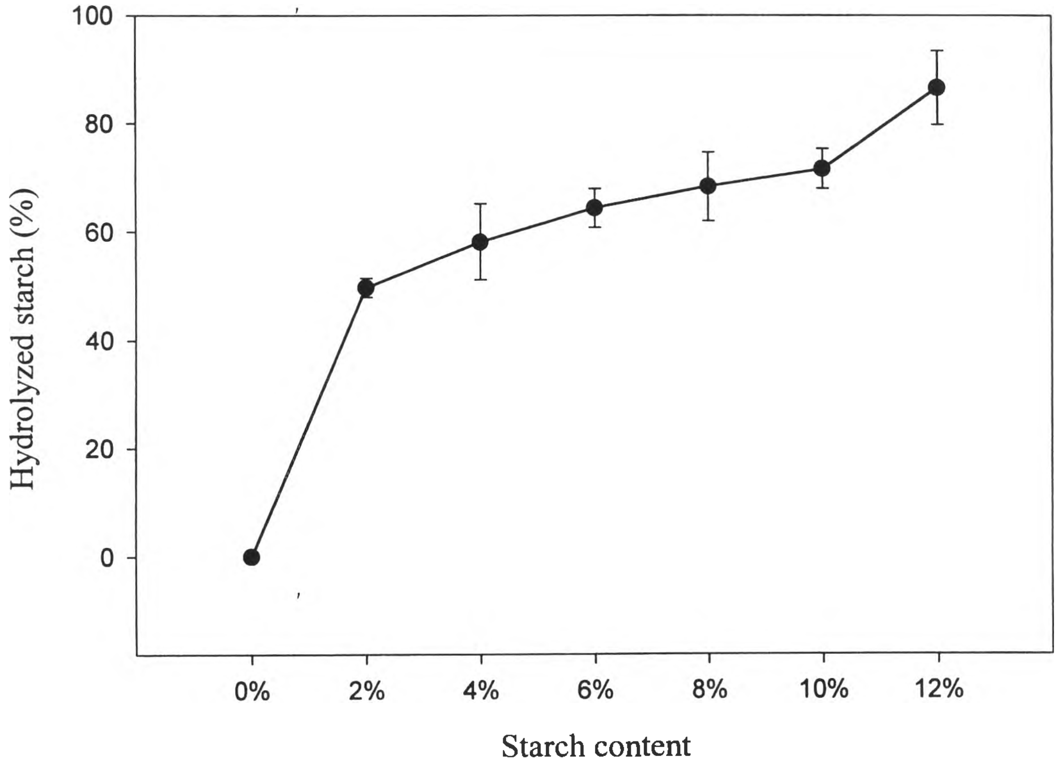

Figure 4.5 Percentages of starch hydrolysis of 50 μm thick film containing 0, 2, 4, 6, 8, 10, and 12 wt% starch hydrolyzed in 5 N HNO_3 at 65°C.

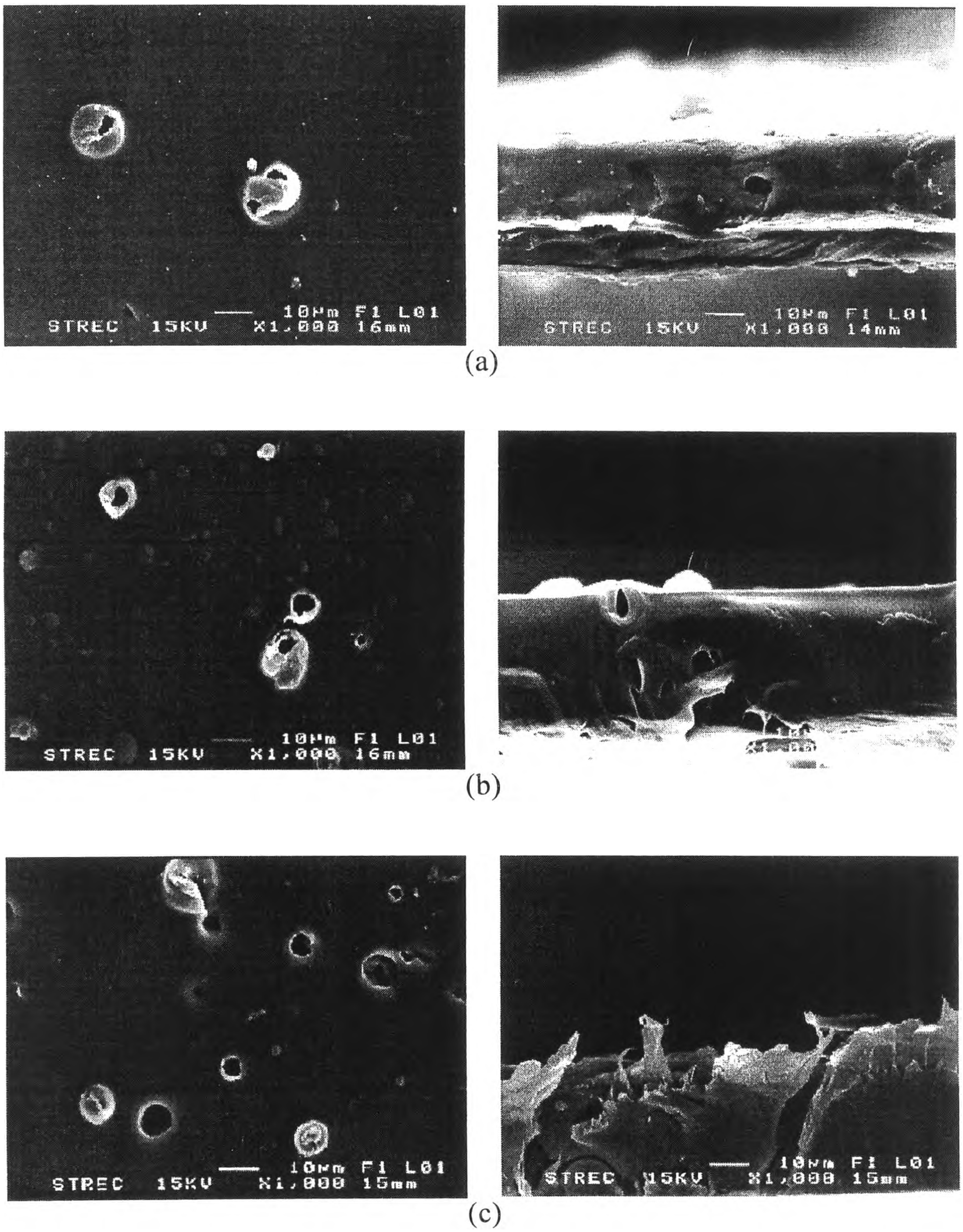

Figure 4.6 SEM micrographs of 50 µm thick films containing (a) 2 wt% starch, (b) 6 wt% starch, and (c) 12 wt% starch hydrolyzed in 5 N HNO_3 at 65°C.

The SEM micrographs in Figure 4.6 clearly support this proposal for higher starch reduction at higher starch loading. At 2 wt% starch content, pores were hardly found in both the surface and the cross-section of the film. The microstructure of the film produced from 2 wt% starch showed a dense, nonporous structure (Figure 4.6a). When the starch level increased to 6 wt%, more pores were formed in both the surface and the cross-section but did not form a porous network (Figure 4.6b). Finally, at 12 wt% starch content, porous structure was observed in both the surface and the cross-sectional image as illustrated in Figure 4.6c. The pores pierced through the whole thickness of the film as seen in the cross-sectional image. Therefore, as the starch content increased from 0-12 wt%, the microstructure of the film changed from dense, nonporous to porous structure.

4.1.1.5 Effect of Film Thickness

The effect of film thickness on the amount of starch removal using 5 N HNO_3 are shown in Figure 4.7. Starch reductions of films with thicknesses of 100 μm and 80 μm were approximately 30% and 50-60%, respectively. The reduction in starch content dramatically increased to 85% for 50 μm thick film. This was thought to be because starch particles were packed closely together in thin film and small thickness helped the solution penetrate easier than in the thick film. Thus, starch reduction increased with decreasing film thickness.

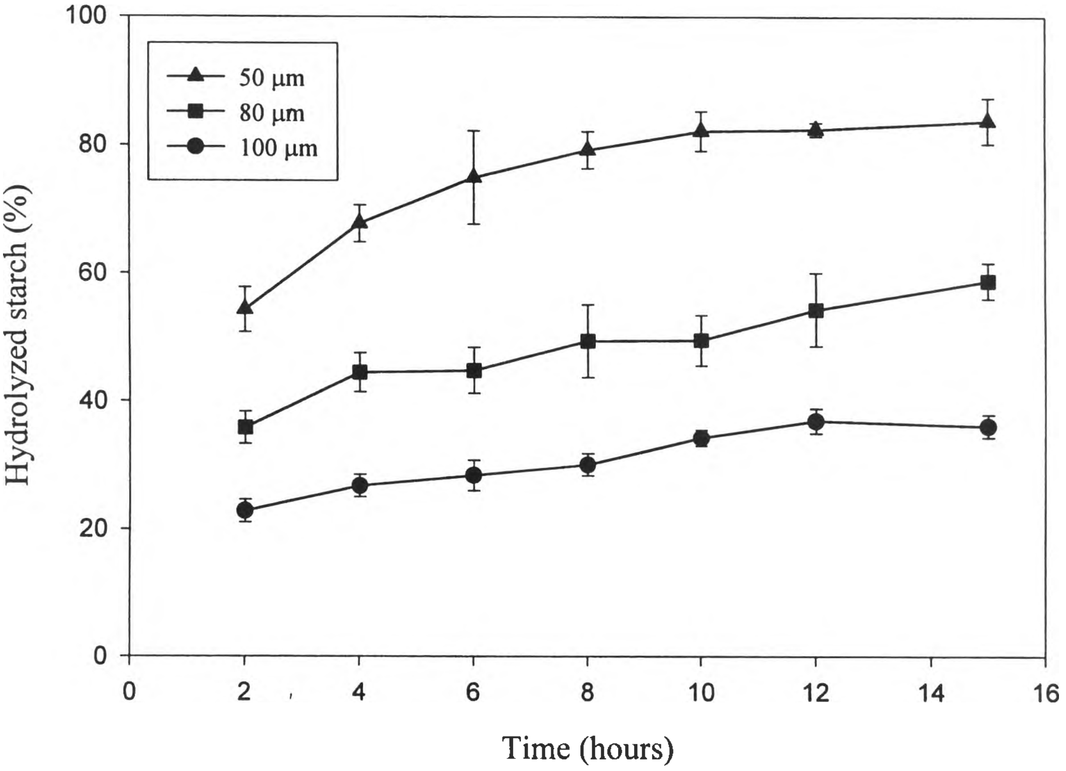

Figure 4.7 Percentages of starch hydrolysis of the films containing 12 wt% starch with varying thicknesses of 50 μm, 80 μm, and 100μm hydrolyzed in 5 N HNO_3 at 65°C as a function of time.

4.1.2 Enzymatic Hydrolysis

Figure 4.8 shows weight loss of the 50 μm thick film containing 12 wt% starch immersed in pH 6.5 acetate buffer at 80°C without enzyme. The weight loss was stable after 6 hours at approximately 1.6 %. This implies that the weight loss of the film hydrolyzed in α-amylase solution was due to both acetate buffer and enzyme. Therefore, the percentage of starch hydrolysis by enzyme was determined by Equation 4.1:

$$\%\ \text{Starch hydrolysis}_{\text{enz}} = \%\ \text{wt loss}_{\text{enz}} - \%\ \text{wt loss}_{\text{w/o enz}} \qquad (4.2)$$

where % Starch $\text{hydrolysis}_{\text{enz}}$ is percentage of starch hydrolysis by enzyme, % wt loss_{enz} is % weight loss with enzyme, and % wt $\text{loss}_{\text{w/o enz}}$ is % weight loss without enzyme. The percentage of starch removal was calculated from Equation 4.3:

$$\%\ \text{starch removal} = \frac{\%\ \text{wt loss}_{\text{st, hyd}}}{\text{initial}\ \%\ \text{starch}} \times 100 \tag{4.3}$$

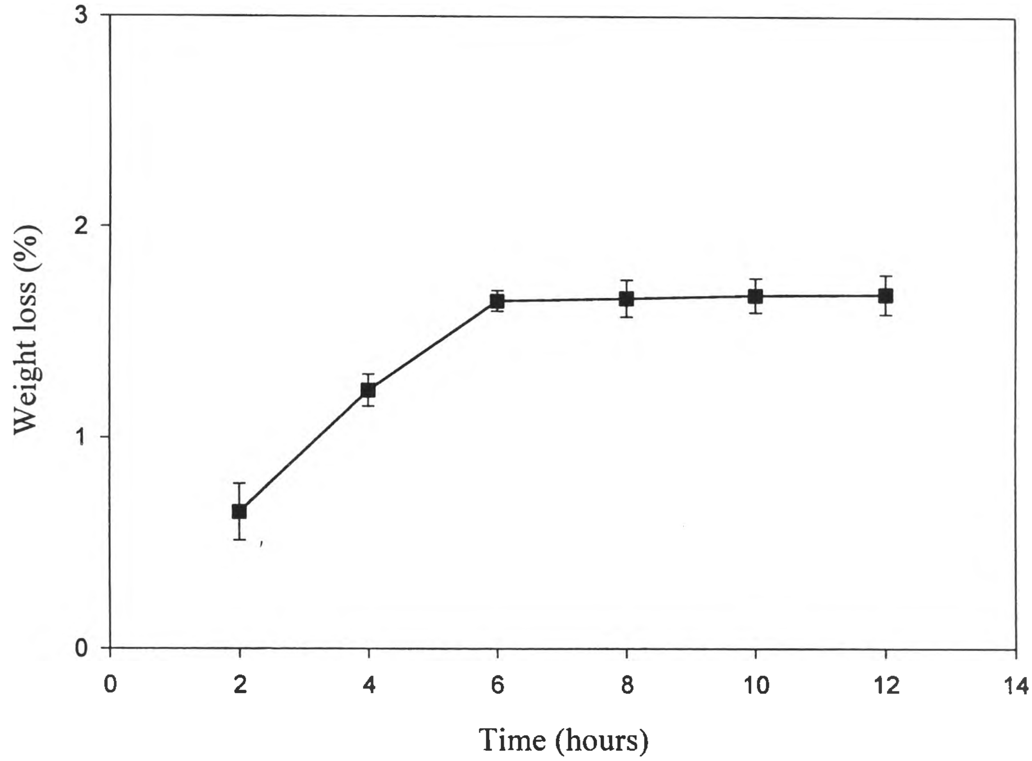

Figure 4.8 Percentage of weight loss of 50 μm thick film containing 12 wt% starch immersed in pH 6.5 acetate buffer at 80°C without enzyme.

Reduction in starch content by α-amylase compared with the reduction by HNO_3 is shown in Figure 4.9. The reduction in starch content by α-amylase increased during the first 8 hours of hydrolysis then remained constant at approximately 35%. The decrease in starch content of 6 wt% starch film of the same thickness (50 μm) hydrolyzed by α-amylase at 37°C was reported by Nakatsuka and Andrady (1992). They found that after prolonged hydrolysis approximately 10% starch was removed as measured by TGA. This value is lower than that of the present work because the hydrolysis was carried out at a lower temperature (37°C) and the initial starch content of the films was lower. In this study, enzymatic hydrolysis showed much lower starch removal than HNO_3 hydrolysis. The results also correlated with SEM micrographs in Figure 4.10a and Figure 4.10b. Both the surface and the cross-section of the α-amylase hydrolyzed film exhibited less pores than the film hydrolyzed in HNO_3 solution.

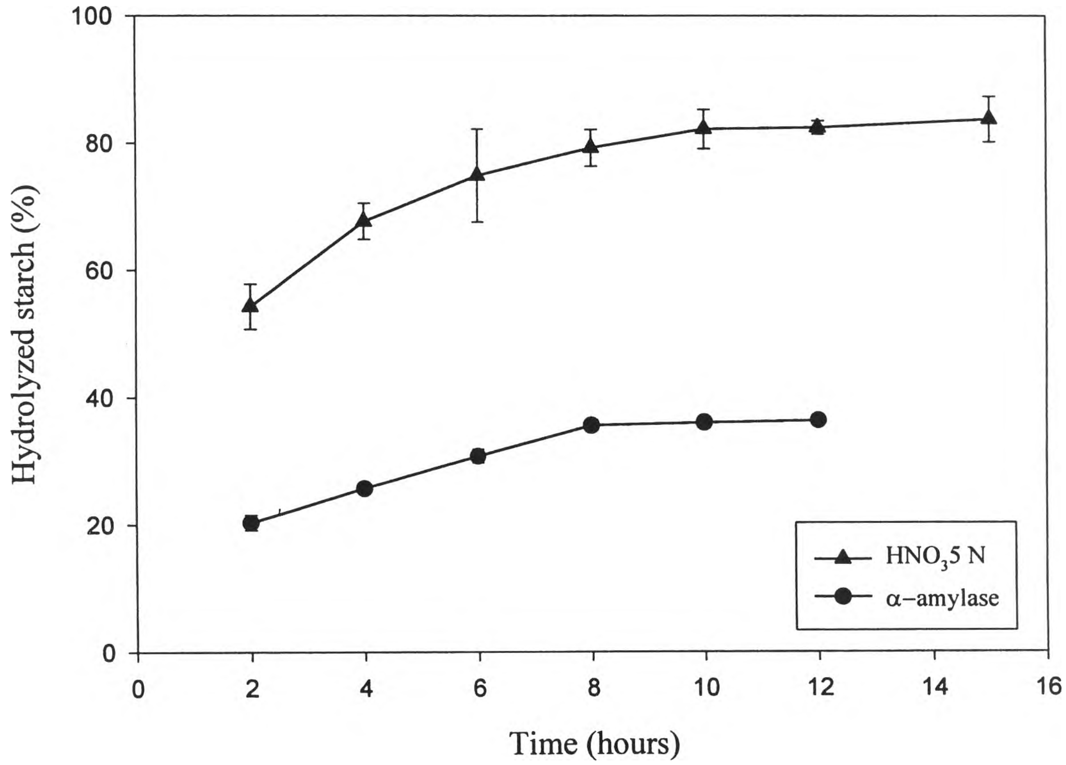

Figure 4.9 Comparison of starch removals from 50 μm thick films containing 12 wt% starch hydrolyzed in 5 N HNO_3 at 65°C and in α-amylase at 80°C.

I 19766CC2

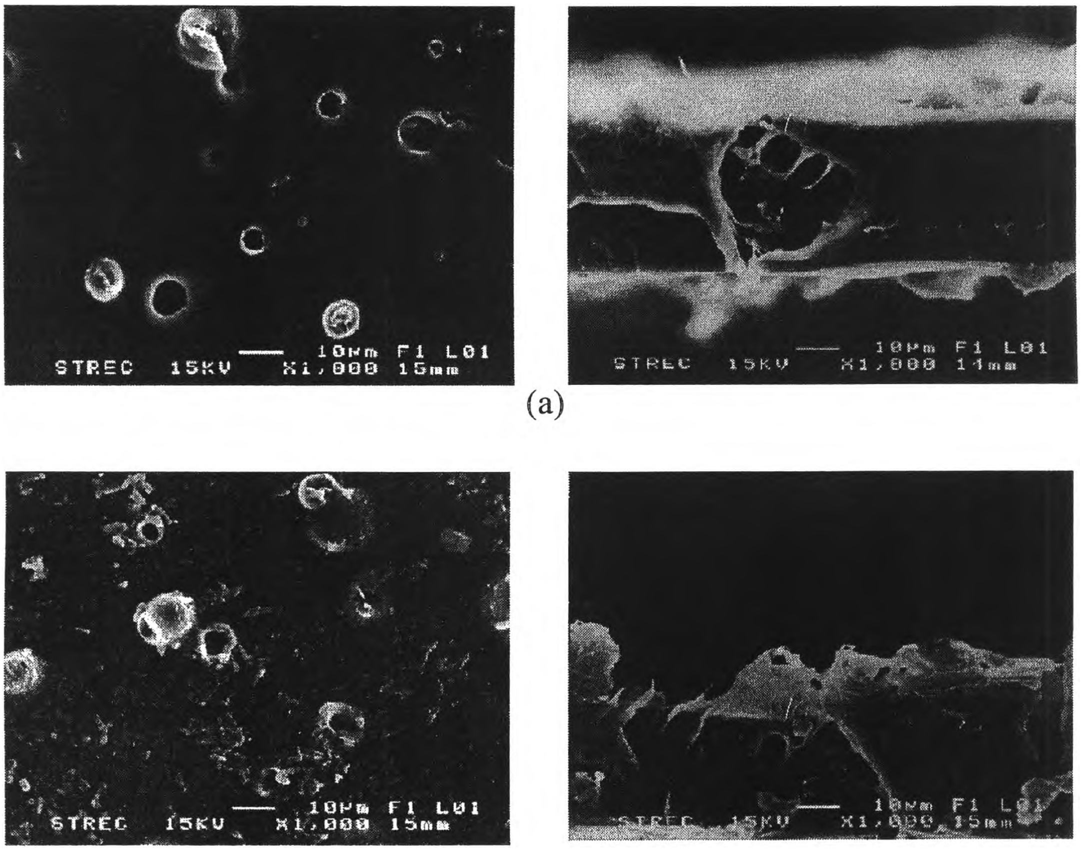

(a)

(b)

Figure 4.10 SEM micrographs of 50 μm thick films containing 12 wt% starch hydrolyzed in (a) 5 N HNO_3 and (b) α-amylase.

4.2 Mechanical Properties

Acidic hydrolysis and enzymatic hydrolysis removed some starch particles from the film matrix resulting in a film having a porous structure. Mechanical properties of the films were determined both before and after starch removal. The properties of interest were tensile stress at break, elongation at break, gloss, and tear resistance.

4.2.1 Tensile Properties

Figure 4.11 shows the tensile stress at break of untreated LDPE/starch film, HNO_3 hydrolyzed film, and α-amylase hydrolyzed film in the machine direction as a function of starch content. A slight decrease in tensile stress at break after both acidic and enzymatic hydrolyzed films was observed. However, the small decreases (1-5%) were not considered significant.

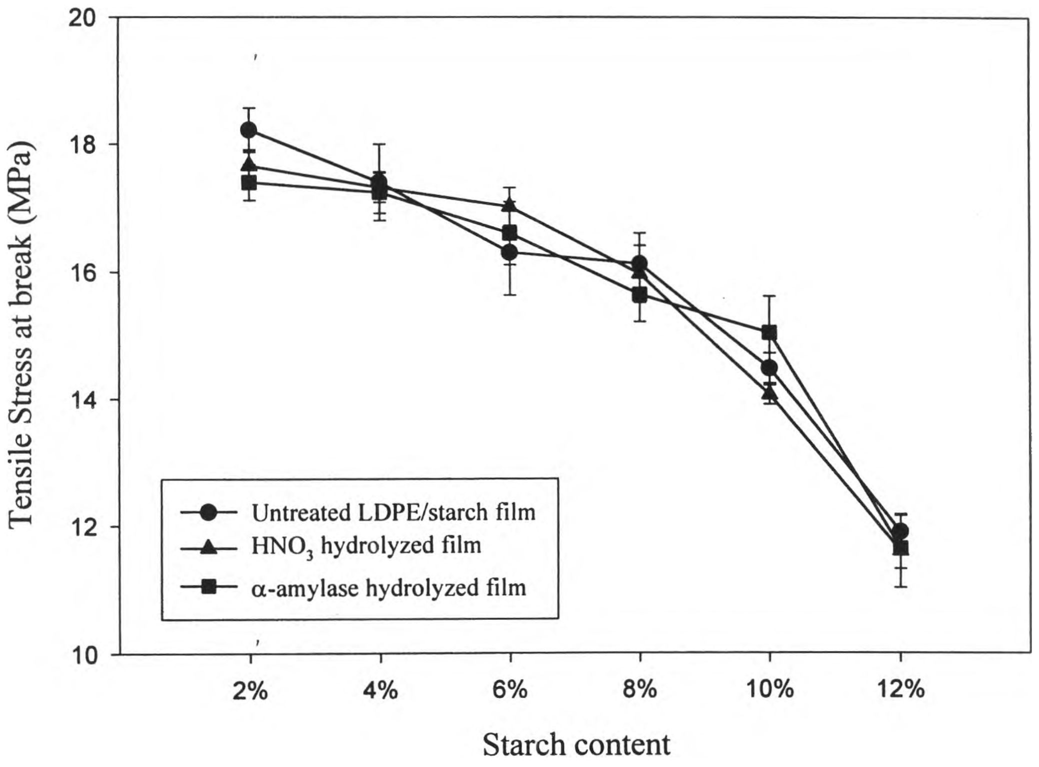

Figure 4.11 Tensile stress at break in machine direction of untreated LDPE/starch film, HNO_3 hydrolyzed film, and α–amylase hydrolyzed film as a function of initial starch content.

A similar slight decrease in elongation at break was found for the porous films (Figure 4.12). In this case, reductions of approximately 12-16%

were observed. The reduction in tensile properties after hydrolysis was due mainly to void formation in the film matrix rather than the effects of HNO_3 solution or α-amylase on the polymer per se.

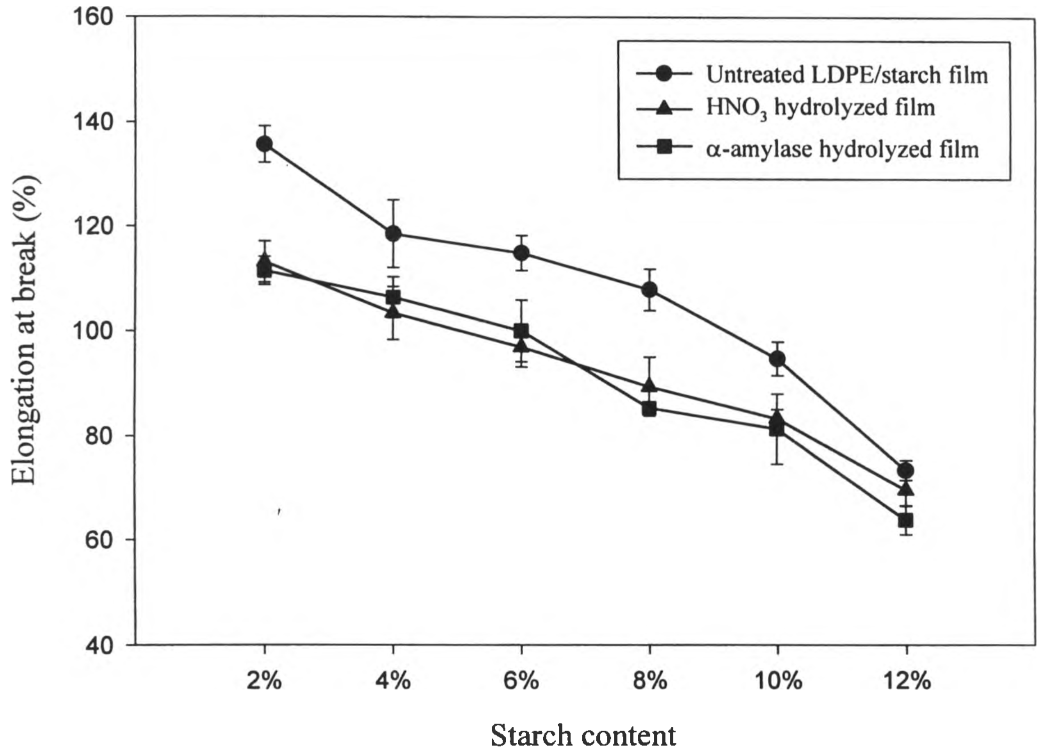

Figure 4.12 Elongation at break in machine direction of untreated LDPE/starch film, HNO_3 hydrolyzed film, and α-amylase hydrolyzed film as a function of initial starch content.

4.2.2 Gloss

Figure 4.13 and Figure 4.14 show gloss values at 60° of untreated LDPE/starch film, HNO_3 hydrolyzed film, and α-amylase hydrolyzed film in machine direction and transverse direction, respectively, as a function of initial starch content. The gloss values of untreated LDPE/starch film decreased in both directions as the starch loading of the film increased. This was because at higher starch contents, films are more opaque and reflect less light than pure LDPE film or films with low starch loading. The gloss values significantly increased after both acidic and enzymatic hydrolysis because some starch had been removed so the film reflected more light than the untreated film. The gloss values also correlated well with the previous results that starch was more effectively hydrolyzed in HNO_3 solution than in α-amylase. This can be seen in both figures that gloss values of HNO_3 hydrolyzed film were higher than those of α-amylase hydrolyzed film.

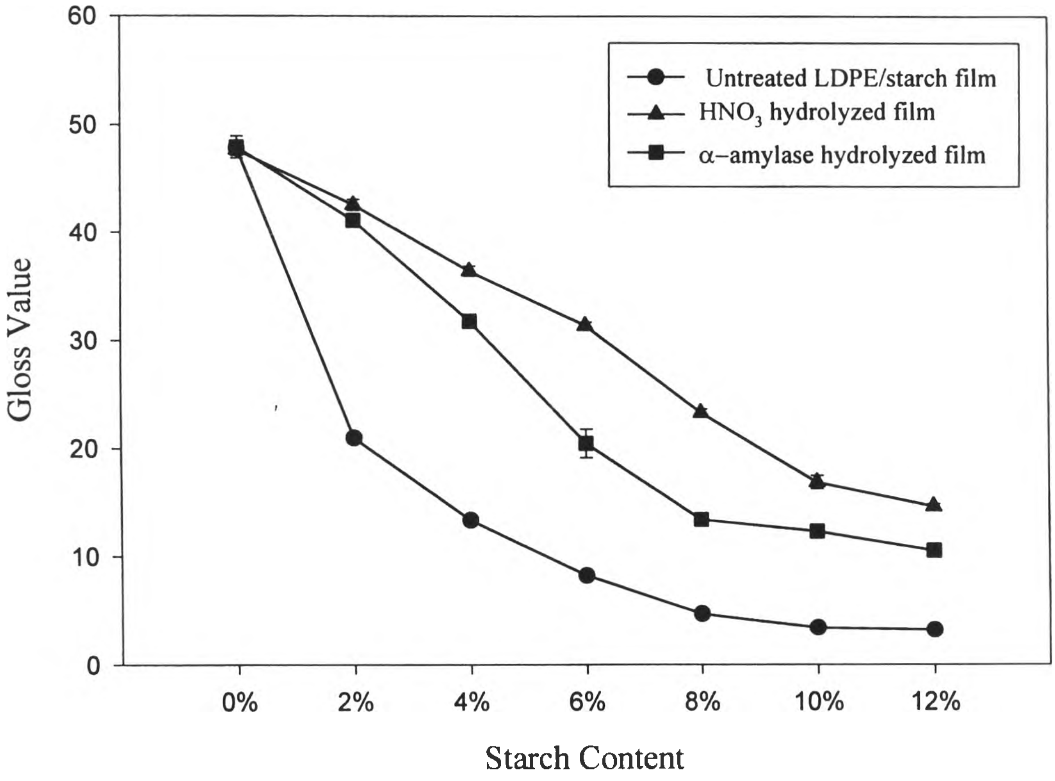

Figure 4.13 Gloss values at 60° of untreated LDPE/starch film, HNO_3 hydrolyzed film, and α-amylase hydrolyzed film in machine direction as a function of starch content.

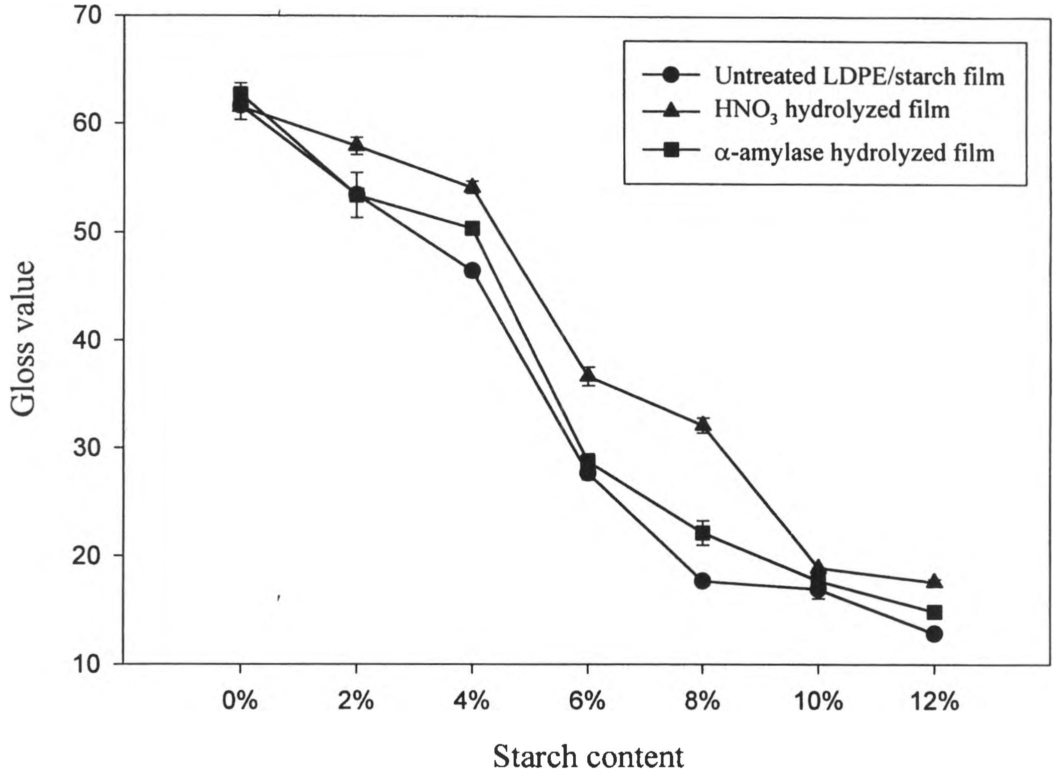

Figure 4.14 Gloss values at 60° of untreated LDPE/starch film, HNO_3 hydrolyzed film, and α-amylase hydrolyzed film in transverse direction as a function of starch content.

4.2.3 Tear Resistance

Figures 4.15 and 4.16 show the tear resistance of untreated LDPE/starch film, HNO_3 hydrolyzed film, and α-amylase hydrolyzed film in both machine and transverse directions. The tear resistance of untreated LDPE/starch film showed peak values at 8 wt% starch content in both directions. This can be explained by the formation of crazes, which act as load-bearing entities, before and after the peak values. At low starch contents, the crazes strengthen the blend leading to an increase in tear resistance. After 8 wt% starch content, the starch particles become closely packed and craze overlapping can occur. This results in a decrease in the actual amount of crazes present and consequently a decrease in tear resistance. This characteristic of the LDPE/starch film disappears after the film has been subjected to acidic or enzymatic hydrolysis. The tear resistance of the films hydrolyzed by HNO_3 and α-amylase showed a significant decrease without peak values due to the discontinuation of the film matrix. Therefore, mechanical properties of the films after hydrolysis decreased due to void formation in the film matrix.

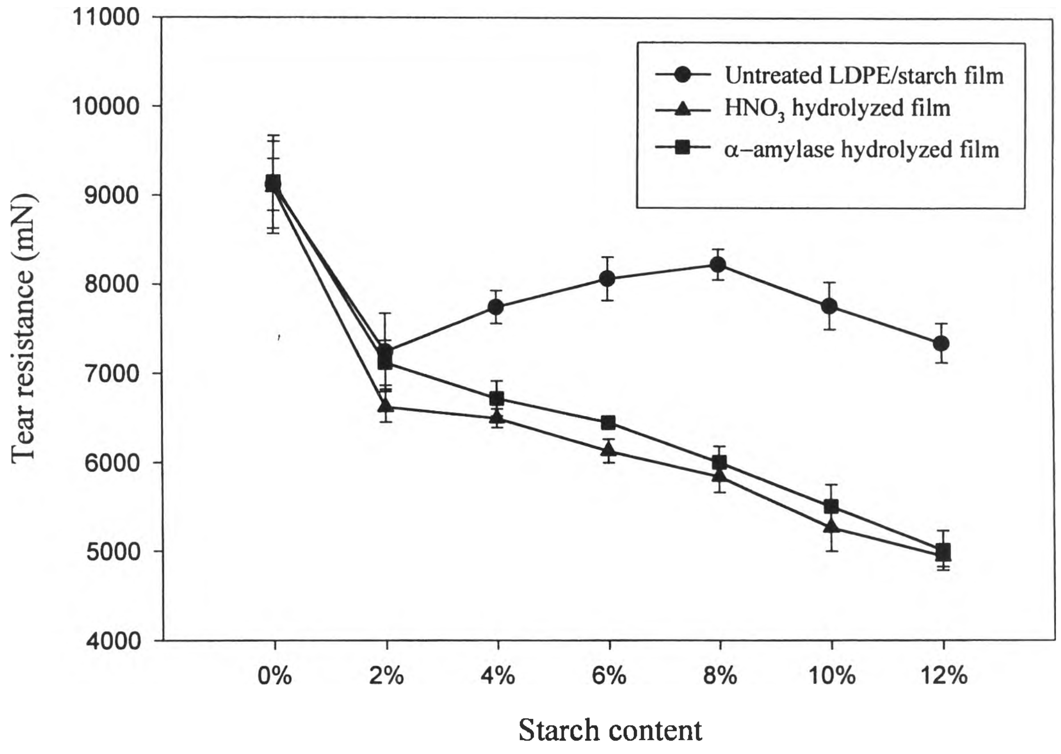

Figure 4.15 Tear resistance in machine direction of untreated LDPE/starch film, HNO_3 hydrolyzed film, and α-amylase hydrolyzed film as a function of initial starch content.

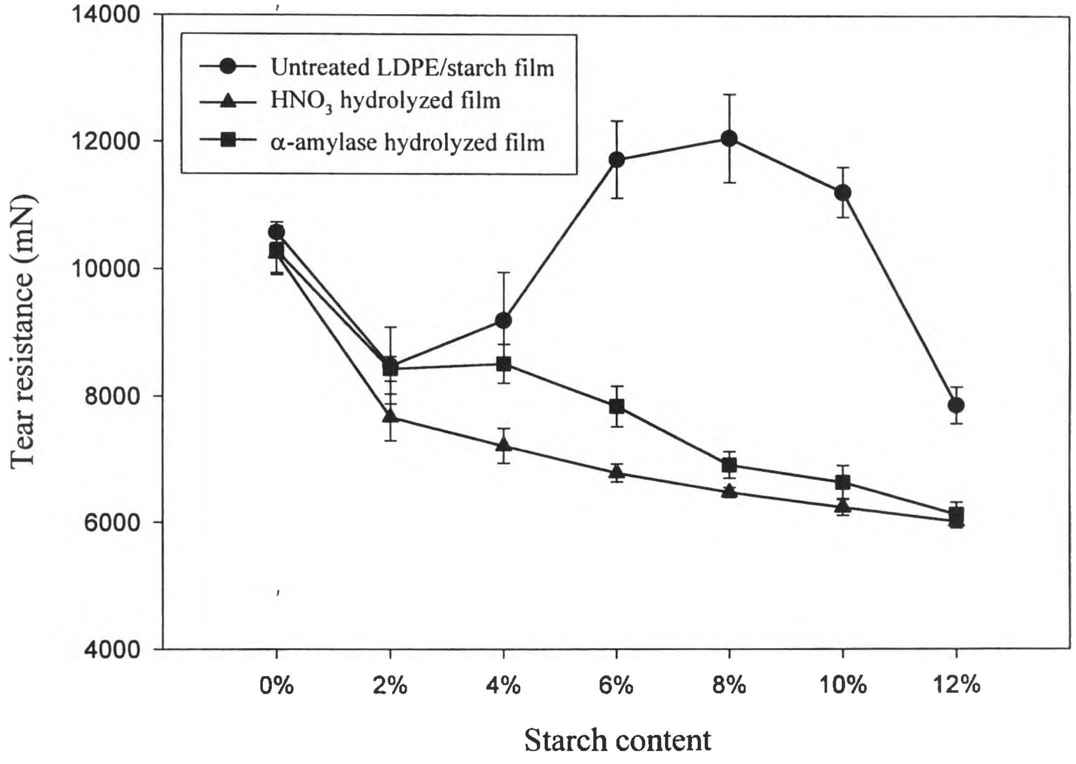

Figure 4.16 Tear resistance in transverse direction of untreated LDPE/starch film, HNO_3 hydrolyzed film, and α-amylase hydrolyzed film as a function of initial starch content.

4.3 Gas Permeability and Selectivity

Figure 4.17 shows the gas permeabilities for N_2, CO_2, C_2H_4, C_3H_8, and C_3H_6 gases through untreated LDPE/starch film as a function of starch content. The gas permeability increased with starch content because gas could easily pass through crazes around starch particles. However, the gas permeabilities for all gases were low and very similar so the films were not considered to be selective.

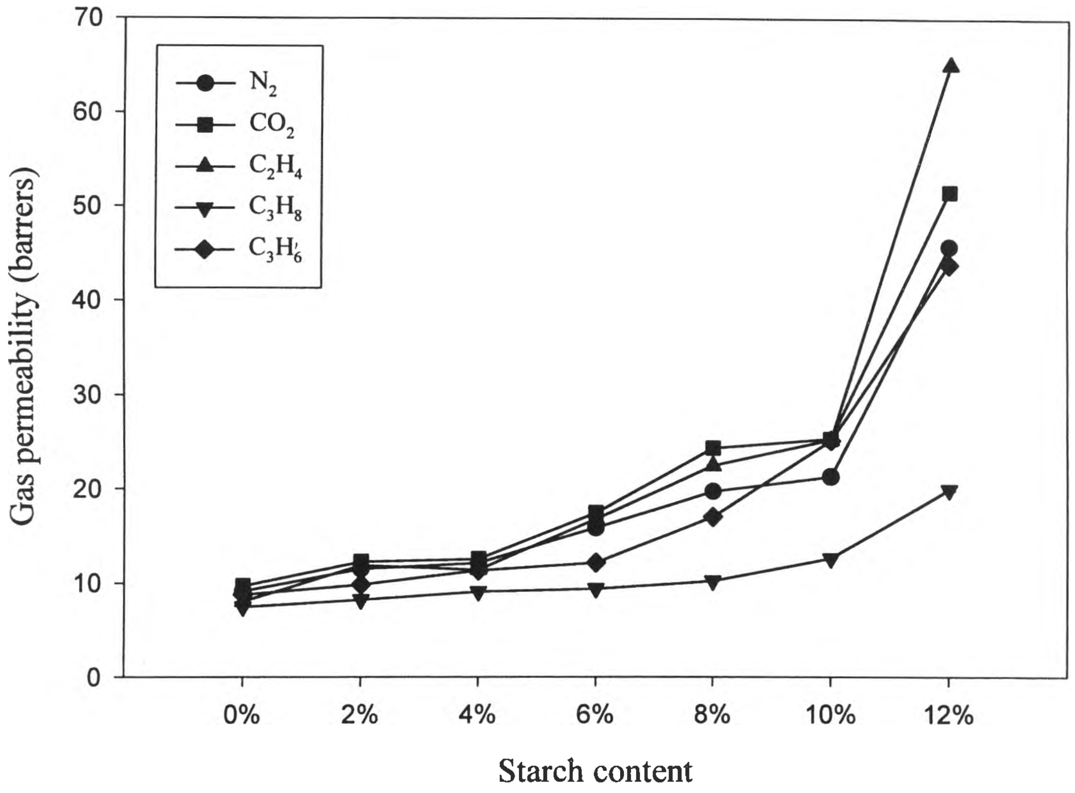

Figure 4.17 Gas permeabilities for N_2, CO_2, C_2H_4, C_3H_8, and C_3H_6 of the untreated LDPE/starch film as a function of initial starch content.

After enzymatic hydrolysis, the porous structure helped enhance the gas permeabilities as shown in Figure 15. The gas permeabilities of the α-amylase hydrolyzed film showed two distinct regions (at 6 wt% starch) depending upon the type of gas used. The higher permeabilities resulted from using N_2, CO_2, and C_2H_4 while the lower values were observed for C_3H_8 and C_3H_6 gases. As previously mentioned, starch particles were most easily hydrolyzed in HNO_3 solution at 65°C. A dramatic increase in gas permeabilities, thus, was found in HNO_3 hydrolyzed film (Figure 16) due to largest number of pores present. This type of film exhibited the highest gas permeabilites and highest selectivities.

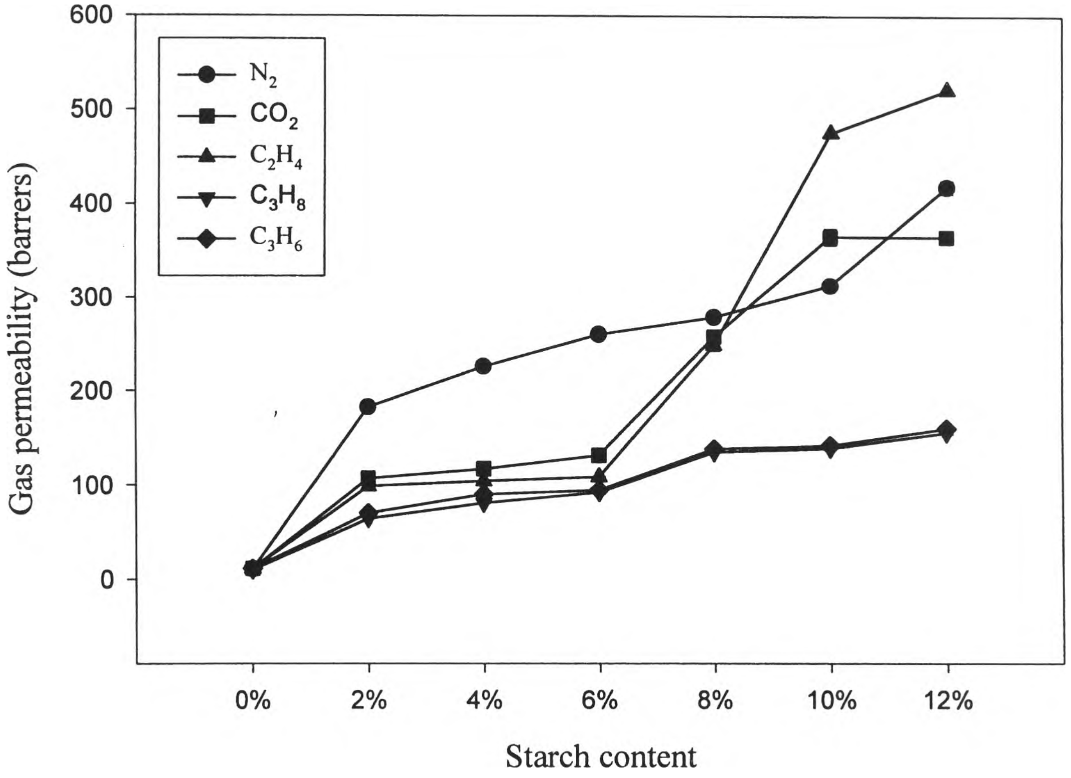

Figure 4.18 Gas permeabilities for N_2, CO_2, C_2H_4, C_3H_8, and C_3H_6 of the α-amylase hydrolyzed film as a function of initial starch content.

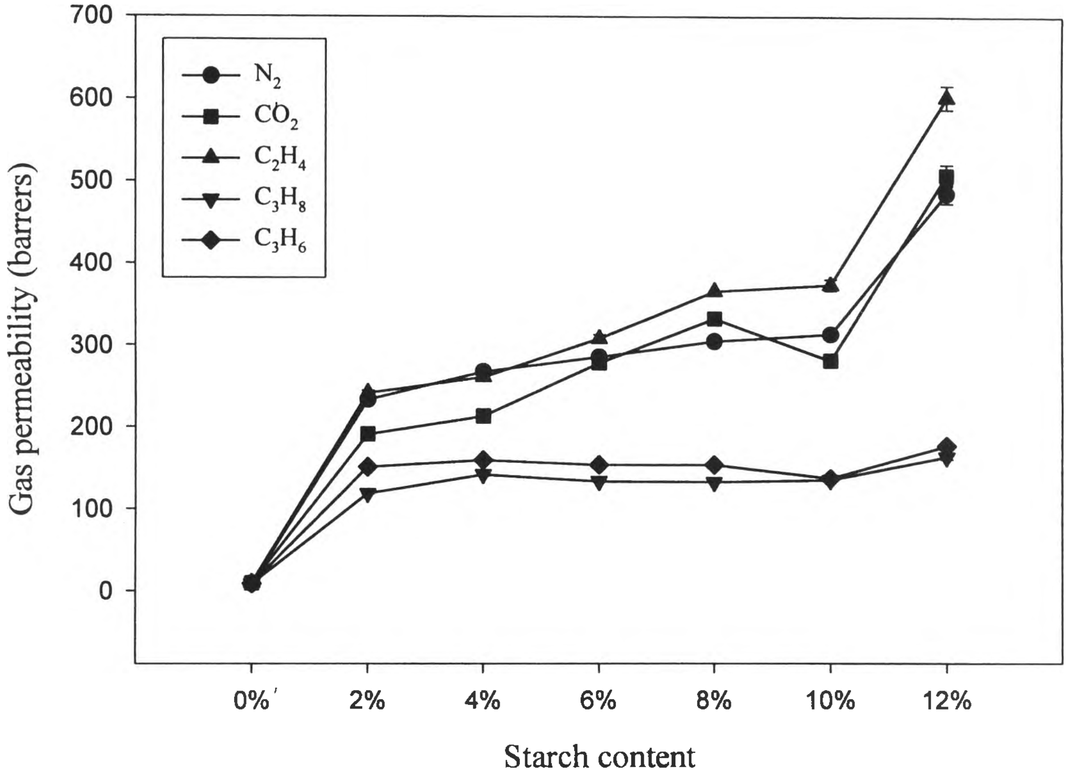

Figure 4.19 Gas permeabilities for N_2, CO_2, C_2H_4, C_3H_8, and C_3H_6 of the HNO_3 hydrolyzed film as a function of initial starch content.

Tables 4.1 and 4.2 summarize the gas permeabilities and selectivities of the films containing 12 wt% starch both before and after hydrolysis. The first table clearly shows that the permeability for all gases was significantly enhanced after hydrolysis especially for the HNO_3 hydrolyzed film. As seen in Table 2, the film hydrolyzed in 5 N HNO_3 has highest selectivity of N_2, CO_2, and C_2H_4 to C_3H_8 and C_3H_6. Therefore, the porous film prepared has a potential for use in industrial gas separation of N_2, CO_2, and C_2H_4 from C_3H_8 and C_3H_6.

Table 4.1 Gas permeabilities of 50 μm thick films with initial starch content of 12 wt%.

Film	Gas permeability (barrers)				
	$P(N_2)$	$P(CO_2)$	$P(C_2H_4)$	$P(C_3H_8)$	P(C3H6)
Untreated LDPE/starch film	45.75	51.61	65.13	19.97	43.84
α-amylase hydrolyzed hilm	417.74	364.74	521.03	155.44	159.51
HNO_3 hydrolyzed film	484.40	506.84	601.50	162.88	176.52

Table 4.2 Selectivity of 50 μm thick films with initial starch content of 12 wt%.

Film	Selectivity					
	$(N_2)/(C_3H_8)$	$(N_2)/(C_3H_6)$	$(CO_2)/(C_3H_8)$	$(CO_2)/(C_3H_6)$	$(C_2H_4)/(C_3H_8)$	$(C_2H_4)/(C_3H_6)$
Untreat LDPE/starch film	2.29	1.04	2.58	1.18	3.26	1.48
α-amylase hydrolyzed hilm	2.69	2.62	2.35	2.29	3.35	3.27
HNO_3 hydrolyzed film	2.97	2.74	3.11	2.87	3.69	3.41